

# Motion Control of Inverted Pendulum Robots Using a Kalman Filter Based Disturbance Observer

Akira SHIMADA\* and Chaisamorn YONGYAI\*

**Abstract:** A high-speed motion control technique for inverted pendulum robots, utilizing instability and a disturbance observer, based on the Kalman filtering technique, is introduced. Inverted pendulums are basically controlled as they do not topple. Shimada and Hatakeyama developed a contrary idea and presented a controller that deliberately off balanced the robot when it moved. To implement the idea, a controller was designed using zero dynamics, which was derived by partial feedback linearization. However, the control system was not robust or sufficiently reliable. Although they presented a revised method using  $H_\infty$  control law, it was complex. Shimada et al. also presented a design method for a disturbance observer using Kalman filtering. This paper presents the latest control technique, combining both control laws to solve the problem, and introduces an application with respect to inverted pendulum robots. It further shows experimental results to confirm its validity.

**Key Words:** inverted pendulum, robot, disturbance observer, Kalman filter, motion control.

## 1. Introduction

This paper introduces a high-speed motion control technique for inverted pendulum robots, based on the concept of instability and a disturbance observer based on Kalman filtering techniques. It is well known that an inverted pendulum is a self-regulated system with a to-and-fro motion similar to the motion of a child swinging an umbrella or a stick [1]–[5]. However, designing a control system for various pendulums has been a challenge since the 1970s. Later, machines based on the same principles were developed for human riding [6],[7], and many biped walking robot designs are also based on this principle. Those inverted pendulums are automatically controlled, as they do not continuously topple.

Shimada and Hatakeyama presented a contrary theory [8]–[10], using a controller that deliberately unbalanced a robot in motion. To implement this concept, a controller was designed using partial feedback linearization [11],[12], which controls only the tilt and orientation angles of the robot. The robot's position is controlled indirectly, rather than directly, although the orientation is directly controlled. In machines designed for humans to ride, which are based on the principle of instability, the unstable states are acquired from operators, not controllers. However, these robots generate unstable states automatically. Applications using the same concept existed [13], but the idea of [8]–[10] was unique, since it was based on the concept of the robots having zero dynamics.

The proposed unstable motion is similar to the sprinting of speed skaters or the motion of a rocket when it starts. Figure 1 illustrates the robot motion with a picture of imaginary robots moving independently. While in motion, the robot tilts, swerves, and makes K-turns. Moreover, it seems to be mov-

ing very fast, but such rapid moves cannot be realized without tilting. This paper discusses only straight motion control, however it introduces a tilt angle control technique for implementing high speed motion. In the future, we expect to see innovative mobile robots being developed using this new control technique based on the concept of instability.

The first and second control systems presented by Shimada and Hatakeyama, which were based on instability, were not robust or sufficiently reliable [8],[9]. The details are as follows. Their first paper [8] presented the basic control scheme based on the instability which achieved the high-speed straight motion. However, it needed two control modes-stable and unstable. Although the unstable control mode implemented the tilt angle control function, it often caused positioning errors. Therefore, the stable control mode, based on a conventional servo control technique, was used to fix the error problem. The second paper [9] introduced a control scheme based on a 3D mathematical model. This scheme achieved straight motion and swerve and pivoting motions as well. However, the positioning error problem remained. To solve this problem, a revised controller, using the  $H_\infty$  control law, was presented, but its structure was too complex [10].

The authors and their colleague [14] presented a design method for a disturbance observer using a Kalman filtering technique. It is well known that disturbance observer based

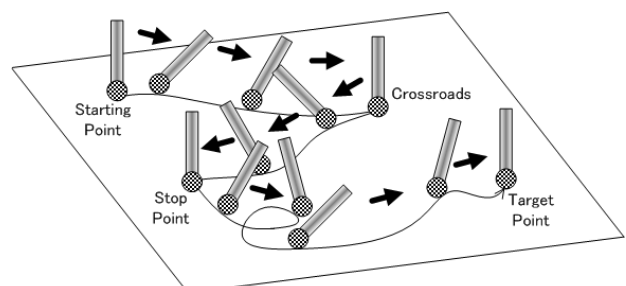


Fig. 1 Motion image of inverted pendulum robot.

\* Department of Electrical System Engineering, Polytechnic University, 4-1-1 Hashimoto-dai, Sagami-hara-shi, Kanagawa 229-1196, Japan  
E-mail: ashimada@u-tec.ac.jp  
(Received October 21, 2008)  
(Revised November 25, 2008)

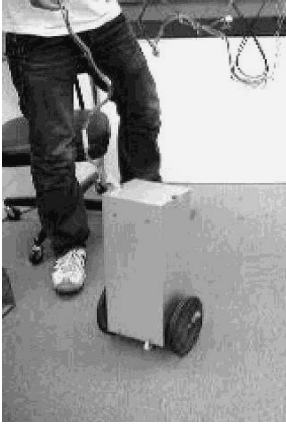


Fig. 2 Exterior view of the robot.

control technology can provide high control performance for a variety of mechanical systems. However, we sometimes encounter involuntary events, as conventional disturbance observer based controllers often cause noisy or unstable motion. One reason is quantization error caused by the low resolution of sensors mounted on the joints of mechanical systems that can inadvertently estimate real disturbance as observation noise. To reconsider the disturbance observer based control technique, this paper introduces a design method based on a steady state Kalman filter design and applies it to inverted pendulum robots. The presented control technique is useful for fixing the error problem simply and to make the robot robust against disturbances.

## 2. Inverted Pendulum Robot

Figure 2 shows the exterior view of an inverted pendulum robot. It is a wheeled inverted pendulum and consists of a body, a pair of wheels, and a contact terminal to detect the body tilt angle. The body includes a pair of DC servo motors with rotary encoders and gear boxes. The base block of the contact terminal is set at the center of the body. The robot body has two small arms with free rollers connected at the terminals of the arms. During the initial stages of development, the robot controller and power amplifier are set outside the robot for convenience and are connected to the motors and sensors via electrical wires. Generally, a two-wheeled pendulum cannot move in a direction inline with the drive shaft without slipping—a property referred to as velocity constraint. A K-turn motion turns the robot. This is a typical problem associated with nonlinear control techniques for non-holonomic systems. This robot is a type of inverted pendulum and does not have an actuator to regulate the tilt angle of the body directly: therefore, it can be considered an under-actuated system. the robot has two types of non-linear characteristics: however, this paper deals with only straight motion control of the inverted pendulum and does not discuss curved motion and K-turn control.

## 3. Coordinate Frames and Modeling of the Inverted Pendulum Robot

The coordinate frames used in this paper are illustrated in Fig. 3.  $\Sigma_F$  refer to the floor coordinate frame,  $\Sigma_V$  is the vehicle coordinate frame.  $\Sigma_B$  is the body coordinate frame, and  $x_v$  is the position of  $\Sigma_V$  from  $\Sigma_F$ .  $\Sigma_B$  is located at the origin of  $\Sigma_V$ . It rotates  $\theta_b$  about the  $Y_V$  axis. The center of mass of the body is

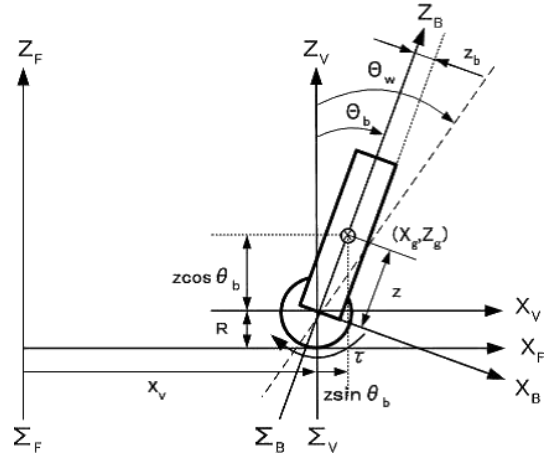


Fig. 3 Variables and coordinate frames.

at  $z$  from  $\Sigma_B$ . Furthermore, the wheel angles are defined as  $\theta_w$ . Normally, the wheel angles should be expressed as  $\theta_{rw}$  and  $\theta_{lw}$  respectively, since the robot has two wheels. However, since this paper treats only straight motion. The relation  $\theta_{rw} = \theta_{lw}$  is assumed and the angles are expressed as  $\theta_w$ .

The equations of motion of the inverted pendulum robot are derived as

$$J_2 \ddot{\theta}_w + J_3 \ddot{\theta}_b \cos \theta_b - J_3 \dot{\theta}_b^2 \sin \theta_b = \tau_s \quad (1)$$

$$J_3 \ddot{\theta}_w \cos \theta_b + J_1 \ddot{\theta}_b - J_3 g/R \sin \theta_b = -\tau_s \quad (2)$$

where  $J_1 = m_b(\frac{4}{3}z^2 + z_b^2)$ , and  $J_2 = R^2(m_b + m_w) + I_w$ ,  $J_3 = m_b z R$ . Further,  $m_b$ ,  $m_w$  refer to the mass of the body and the wheel. It is assumed that  $z$  is half of the body height, the width is  $2z_b$ , and the radius of the wheels is  $R$ .  $\theta_w$  is the wheel angle.  $\theta_b$  is the tilt angle of the body, and  $\tau_s$  is the driving torque. Using the equation of motion, the nonlinear state equation is derived as

$$\begin{bmatrix} \dot{\theta}_w \\ \dot{\theta}_b \\ \ddot{\theta}_w \\ \ddot{\theta}_b \end{bmatrix} = \begin{bmatrix} \dot{\theta}_w \\ \dot{\theta}_b \\ f_3 \\ f_4 \end{bmatrix} + \begin{bmatrix} 0 \\ 0 \\ g_3 \\ g_4 \end{bmatrix} \tau_s \quad (3)$$

where  $Det(\theta_b) = J_1 J_2 - J_3^2 \cos^2 \theta_b$ ,  
 $f_3 = \frac{J_1}{Det(\theta_b)} (J_3 \sin \theta_b \cdot \dot{\theta}_b^2) - \frac{J_3 \cos \theta_b}{Det(\theta_b)} (J_3 g/R \cdot \sin \theta_b)$ ,  
 $f_4 = \frac{-J_3 \cos \theta_b}{Det(\theta_b)} (J_3 \sin \theta_b \cdot \dot{\theta}_b^2) + \frac{J_2}{Det(\theta_b)} (J_3 g/R \cdot \sin \theta_b)$ ,  
 $g_3 = \frac{J_1 + J_3 \cos \theta_b}{Det(\theta_b)}$ ,  $g_4 = \frac{-J_3 \cos \theta_b - J_2}{Det(\theta_b)}$ .

## 4. Kalman Filter Based Identity Disturbance Observer

### 4.1 Identity Disturbance Observer [15]

Now, using the conventional linearization of Eqs. (1) and (2), the continuous state and output equations are derived as

$$\dot{x}_s = A_c \dot{x}_s + B_c u_s - B_s d \quad (4)$$

$$y_s = C_s x_s \quad (5)$$

where  $x_s = [\theta_w, \theta_b, \dot{\theta}_w, \dot{\theta}_b]^T$ ,  $u_s = \tau_s$ ,  $y_s = [\theta_w, \theta_b]^T$ , and  $d$  means equivalent input disturbance.

$$A_s = \begin{bmatrix} 0 & 0 & 1 & 0 \\ 0 & 0 & 0 & 1 \\ 0 & -\frac{J_3^2 g}{Det \cdot R} & 0 & 0 \\ 0 & \frac{J_2 J_3 g}{Det \cdot R} & 0 & 0 \end{bmatrix}, \quad B_s = \begin{bmatrix} 0 \\ 0 \\ \frac{J_1 + J_3}{Det} \\ -\frac{J_2 + J_3}{Det} \end{bmatrix}$$

$$C_s = \begin{bmatrix} 1 & 0 & 0 & 0 \\ 0 & 1 & 0 & 0 \end{bmatrix}$$

$$Det = \max(Det(\theta_b)) = J_1 J_2 - J_3^2.$$

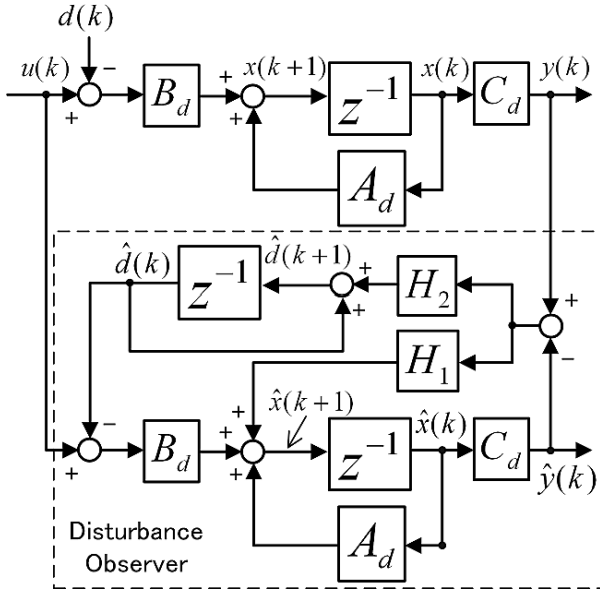


Fig. 4 A Block diagram of the digital identity disturbance observer.

It means that  $\sin \theta_b$ ,  $\cos \theta_b$ , and  $\dot{\theta}_b^2$  are approximated by  $\theta_b$ , 1, and 0, respectively.

Next, they are converted to a discrete state equation and output equation as

$$x_s(k+1) = A_d x_s(k) + B_d u_s(k) - B_d d(k) \quad (6)$$

$$y_s(k) = C_d x_s(k) \quad (7)$$

where the dimension of each coefficient matrix  $A_d$ ,  $B_d$ ,  $C_d$  is the same as the dimension of the above continuous system. Furthermore, it is assumed that the disturbance satisfies  $\dot{d} = 0_{m \times 1}$  and the condition is replaced as  $d(k+1) = d(k) \in R^m$ . The characters  $k, k+1$  in ( ) mean  $t = kT, (k+1)T$ .

Next, the revised state variable vector  $x_o(k) = [x_s(k)^T, d(k)^T]^T$  is defined, including the disturbance. Thus, the extended discrete state equation and output equations are derived as

$$x_o(k+1) = A_o x_o(k) + B_o u_s(k) \quad (8)$$

$$y_o(k) = C_o x_o(k) \quad (9)$$

$$\text{where } A_o = \begin{bmatrix} A_d & -B_d \\ 0 & I \end{bmatrix}, B_o = \begin{bmatrix} B_d \\ 0 \end{bmatrix}, C_o = \begin{bmatrix} C_d & 0 \end{bmatrix}.$$

From Eqs. (8) and (9), the identity disturbance can be designed as

$$\hat{x}_o(k+1) = A_o \hat{x}_o(k) + B_o u(k) + H \{y_o(k) - \hat{y}_o(k)\} \quad (10)$$

$$\hat{y}_o(k) = C_o \hat{x}_o(k) \quad (11)$$

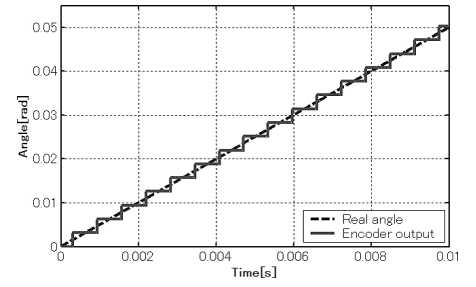
where  $H = [H_1^T, H_2^T]^T$  is the gain matrix of the observer. Figure 4 shows a block diagram of the control plant and the presented disturbance observer, which is described using the components in  $A_o$ ,  $B_o$ ,  $C_o$ .

#### 4.2 Design of a Kalman Filter Based Identity Disturbance Observer

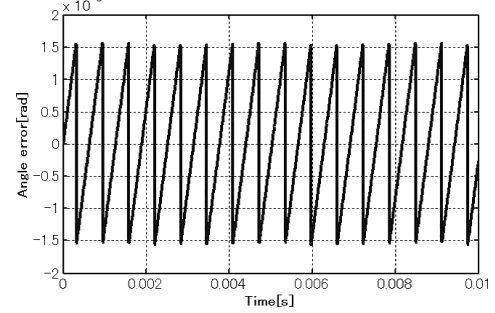
Assuming that white system noise  $\omega(k) \in R^n$  and white sensor noise  $\epsilon(k) \in R^l$  are added to the extended system, Eqs. (8), (9), the extended system equations are modified as

$$\bar{x}(k+1) = \bar{A}_d \bar{x}(k) + \bar{B}_d u_s(k) + \omega(k) \quad (12)$$

$$y(k) = \bar{C}_d \bar{x}(k) + \epsilon(k) \quad (13)$$



(a) Example of actual angle and encoder output



(b) Example of sensing error

Fig. 5 Encoder output and angle error.

where  $E[\omega(k)] = 0$ ,  $E[\epsilon(k)] = 0$ ,  $E[\omega(k)\epsilon(j)^T] = 0$ ,  $E[\omega(k)\omega(j)^T] = Q_{ob}\delta_{k,j}$ ,  $E[\epsilon(k)\epsilon(j)^T] = R_{ob}\delta_{k,j}$ ,  $Q_{ob} \geq 0$ ,  $R_{ob} > 0$ .

$$J = E[(\bar{x}(k) - \hat{\bar{x}}(k))^T (\bar{x}(k) - \hat{\bar{x}}(k))] \quad (14)$$

$$H = -\bar{A}_d P \bar{C}_d^T (R_{ob} + \bar{C}_d P \bar{C}_d^T)^{-1} \quad (15)$$

$$P = Q_{ob} + \bar{A}_d P \bar{A}_d^T - \bar{A}_d P \bar{C}_d^T (R_{ob} + \bar{C}_d P \bar{C}_d^T)^{-1} \bar{C}_d P \bar{A}_d^T \quad (16)$$

A Kalman filter is a type of estimator that minimizes the variance of the estimation error  $J$ , which is expressed as Eq. (14). In the case of a steady state Kalman filter, the forms of the equations are the same as those of a conventional identity observer. Thus, the steady state Kalman filter based disturbance observer is expressed as Eqs. (10) and (11). The Kalman gain matrix,  $H = [H_1^T, H_2^T]^T$  is designed to minimize  $J$  using Eqs. (15) and (16). Figure 5 (a) shows the relation between the actual angle and the encoder output, and (b) shows the sensing error used to estimate the system covariance.

#### 5. Movement Controller Design

To implement the proposed movement control system, the control input  $u_s(k)$  should consist of the nonlinear input  $u(k)$  and the disturbance estimate  $\hat{d}(k)$ . This means modifying the nonlinear control plant to the equivalent linear plant using  $\hat{d}(k)$  to cancel the external disturbance and the effects of modeling error.

$$u_s(k) = u(k) + \hat{d}(k) \quad (17)$$

It is well known that an equivalent linear system related to inverted pendulums is not controllable except at the equilibrium points. Therefore, the controller cannot regulate all the state variables and make all the system poles stable in the global range concurrently. Thus, this paper discusses the movement control of a few variables while the robot is in motion. However, since it is difficult to design a nonlinear feedback controller with digital control theory, the subsequent controller is

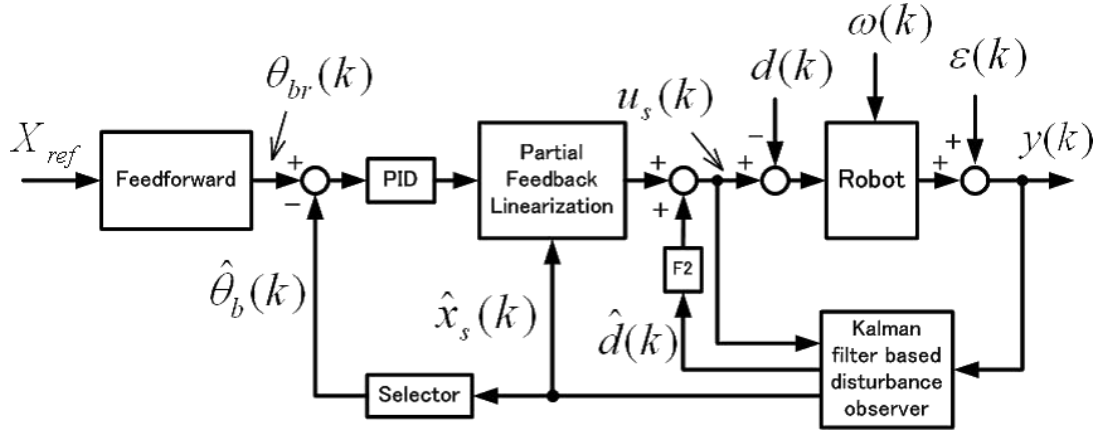


Fig. 6 The block diagram of the control system.

designed using continuous theory. In practice, only  $\ddot{\theta}_b$  is partially linearized by Eq. (18), as  $\ddot{\theta}_b = v$  is realized [11],[12].

$$u(k) = \frac{J_2 J_3 g}{R(J_2 + J_3)} \theta_b(k) - \frac{Det}{J_2 + J_3} v(k) \quad (18)$$

Instead of the implementation of  $\ddot{\theta}_b = v$ , the remaining part, which is the third row of the matrix  $A_d$ , is modified to  $\ddot{\theta}_w = f_5 \theta_b + g_5 v$  where  $f_5 = \frac{J_3 g}{Det \cdot R} \frac{J_1 J_2 + J_2 J_3 - J_3(J_2 + J_3)}{J_2 + J_3}$ ,  $g_5 = -\frac{J_1 + J_3}{J_2 + J_3}$ .

When  $v$  is small, the second term can be neglected and the equation approximated as  $\ddot{\theta}_w = f_5 \theta_b$ . It is known that this equation expresses a kind of zero dynamics. When a PID control law  $v = k_p(\theta_{br} - \theta_b) + k_i \int_0^t (\theta_{br} - \theta_b) dt - k_d \dot{\theta}_b$  is used,  $\theta_b$  converges to  $\theta_{br}$ . Thus, Eq. (19) is obtained, which means that the tilt angle  $\theta_b$  can be controlled if the acceleration of the robot  $\ddot{\theta}_w$  is to be controlled on track  $\ddot{\theta}_{wr}$ .

$$\theta_{br} = \frac{1}{f_5} \ddot{\theta}_{wr} \quad (19)$$

To control the position of the robots, to set it in motion, the acceleration reference  $a_r$  is calculated from the second order derivative of the position reference  $x_r$ , which is a function of time. Next,  $\ddot{\theta}_w = a_r/R$  and  $\theta_{br}$  are derived from Eq. (19). The resultant control law indicates an indirect position control based on instability. Figure 6 shows the block diagram of the control system.

## 6. Experimental Result

This section presents the experimental results for evaluating the control performance. Figure 7 describes the hardware struc-

Table 1 Physical parameters of the inverted pendulum.

Mass of the body $m_b$	8.8 (kg)
Half of height of the body $z$	0.20 (m)
Half of width of the body $z_b$	$7.5 \times 10^{-2}$ (m)
Radius of the wheel $R$	$8.5 \times 10^{-2}$ (m)
Mass of the wheel $m_w$	0.6 (kg)

Table 2 Control parameters.

Proportional gain $k_p$	$7.20 \times 10^2$ (1/s <sup>2</sup> )
Integral gain $k_i$	2.80 (1/s <sup>3</sup> )
Derivative gain $k_d$	8.50 (1/s)
Sample rate: $T_{samp}$	1.0 ms
Covariance $Q_{ob}$	$diag(1.0e6, 1.0e5, 2.0e3, 1.0e3, 2.0e5)$
Covariance $R_{ob}$	$diag(1.0e-2, 1.0e-2)$

Note: The character “e \* ” means “ $\times 10^{**}$ ”.

ture of the experimental control system. The inverted pendulum robot is driven by a pair of 140 W DC servo motors, which are installed in the body of the robot. The controller was designed using MATLAB/Simulink/RealtimeWorkshop program, produced by MathWorks Inc. The tilt angle and the wheel angles are detected by rotary encoders manufactured by Microtech Laboratory Inc. They are mounted in the robot's body. The program is transferred to a controller S-box produced by MTT Inc. in Japan. The control program runs every 1 ms.

The physical and control parameter values used in the experiment are shown in Tables 1 and 2, respectively. They were collected from the data of real robots under development.

Figure 8 shows the actual experimental results related to the control system. Basically, the figures indicate that the presented control law is suitable as intended. The top line shown in Fig. 8(a) illustrates the position reference  $x_r$  with a dotted line, and the real position  $x (= R \cdot \theta_w)$  of the robot with a solid line. The waveform of  $x$  tracks  $x_r$  fairly well, departing from  $x_r$  once from 22.5 s to 23 s because of a disturbance given to the robot manually. Note that  $x$  returns to  $x_r$  from 23 s to 25 s. The second line of the figure shows the tilt angle reference  $\theta_{br}$  and real tilt angle  $\theta_b$ , and  $\theta_b$  tracks  $\theta_{br}$  very well, which means the tilt

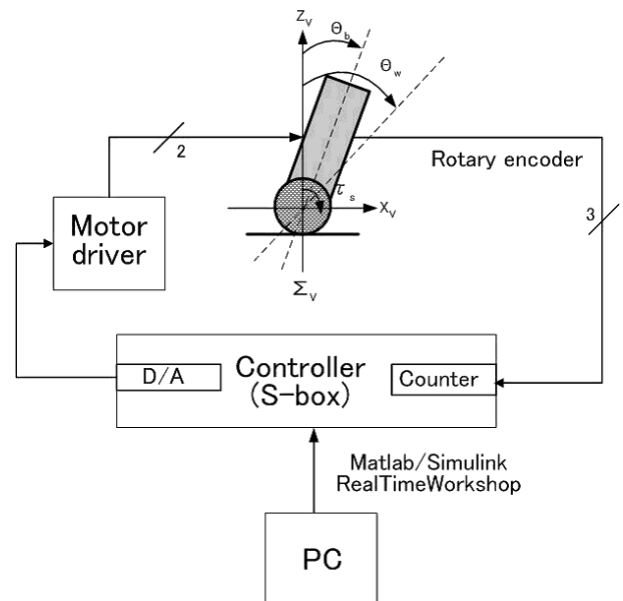
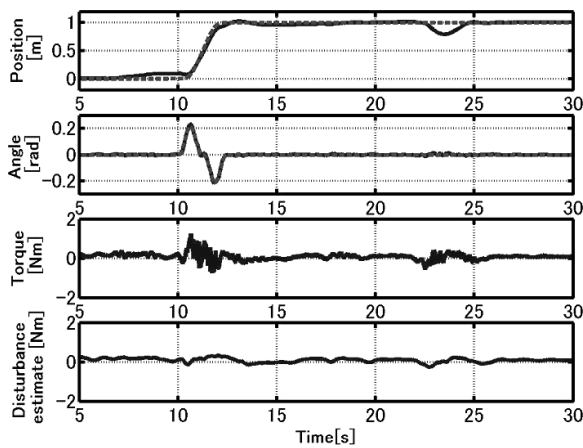
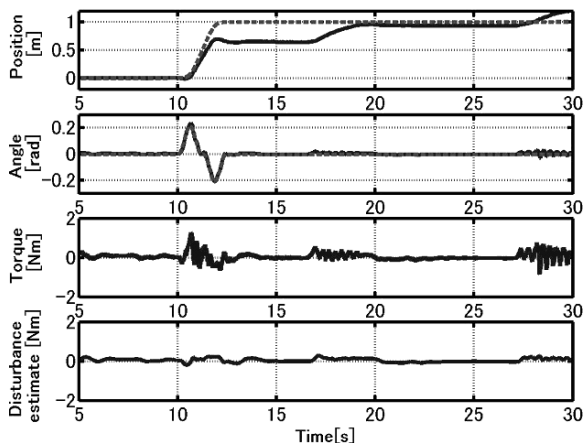


Fig. 7 The system hardware structure.





(a) with feedback of estimated disturbances



(b) without feedback of estimated disturbances

Fig. 8 Experimental results of straight motion.

angle control is executed successfully. It seems that the control law based on tilt angle control realizes the intended high-speed motion control. The third line of the figure shows the actual control input torque  $\tau$  and the fourth line of the figure describes the disturbance estimate.

Figure 8 (b) shows another experimental result for the control system without disturbance estimate feedback. The top line of Fig. 8 (b) illustrates the  $x_r$  and  $x (= R \cdot \theta_w)$ . The waveform of  $x$  does not track  $x_r$  well, although the tilt angle control performs reasonably well.  $x$  does not track  $x_r$  from about 10.5 s to 17 s and from 17 s to about 18.5 s the operator provides a manual disturbance to support the robot, and the robot almost tracks the position reference. However, after 28 s, the robot departs due to the another manual disturbance.

Figures 9 and 10 show sequential photographs of the robot's motion—the same motions as in Figs. 8 (a) and (b). They show that the intended high-speed motions are realized.

## 7. Conclusion and Future Work

This paper discussed the latest control technique for two-wheeled inverted pendulum robots using instability with a Kalman filter based disturbance observer. It utilized partial linearization feedback and the cancellation by the disturbance estimate feedback. The experimental results demonstrated that the proposed concept works well. This result is better than previous results [8]–[10] and the control technique is expected to help development of innovative mobile robots that can move

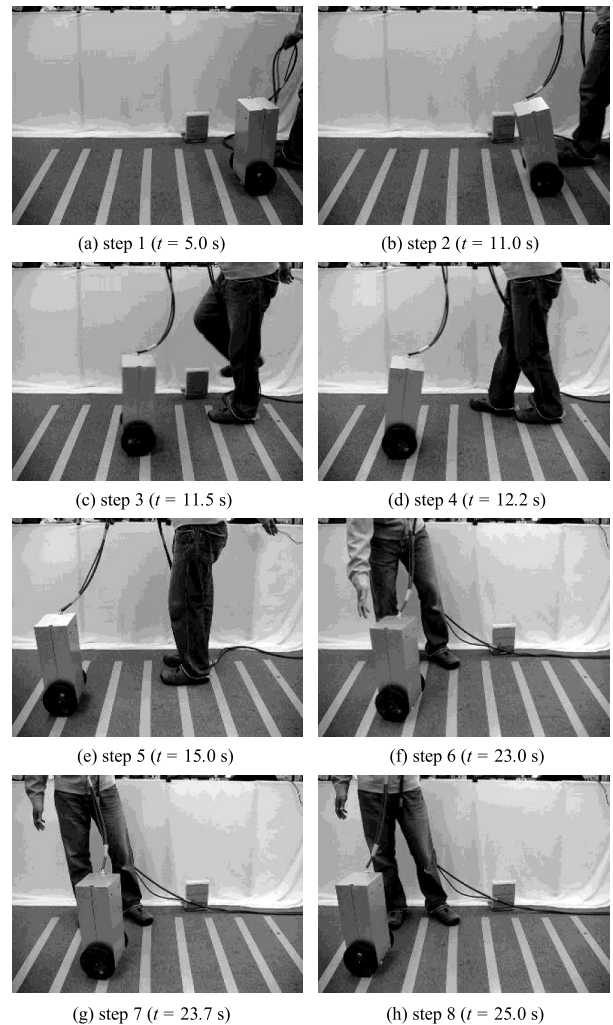


Fig. 9 Sequential photographs of movement control with Kalman filter based disturbance estimate feedback.

quickly.

## Acknowledgments

The authors acknowledge the contribution by the members of Microtech Laboratory Inc.

## References

- [1] Rogerugist: Experiment to stand up dolls, *Mall to Physics*, pp.77–84, Iwanami, 1963 (in Japanese).
- [2] K. Furuta, T. Okutani, and H. Sone: Computer control of a double inverted pendulum, *Computer and Electrical Engineering*, Vol.5, pp.67–84, 1978.
- [3] P. Albertos, P.A. Perez, R. Strietzel, and N. Mort: *Control Engineering Solutions: A Practical Approach*, IET, 1997.
- [4] N.R. Prasad, S.T. Balfour, H.T. Nguyen, and E.A. Walker: *A First Course in Fuzzy and Neural Control*, CRC Press, 2002.
- [5] S.K. Spurgeon and C. Edwards: *Sliding Mode Control: Theory and Applications*, Taylor & Francis, 1998.
- [6] Segway Inc.: <http://www.segway.com/>
- [7] D.L. Kamen, R.R. Ambrogio, R.J. Duggan, R.K. Heinzmann, B.R. Key, A. Skoskiewicz, and P.K. Kristal: Transportation Vehicles and Methods, U.S. Patent No.5971091, 1999.
- [8] A. Shimada and N. Hatakeyama: High-speed motion control of inverted pendulum robots, *9th IEEE International Workshop on Advanced Motion Control—AMC '06*, pp.307–310, 2006.
- [9] N. Hatakeyama and A. Shimada: Movement control using zero dynamics of two-wheeled inverted pendulum robot, *Trans. SICE*, Vol.44, No.3, pp.252–259, 2008 (in Japanese).

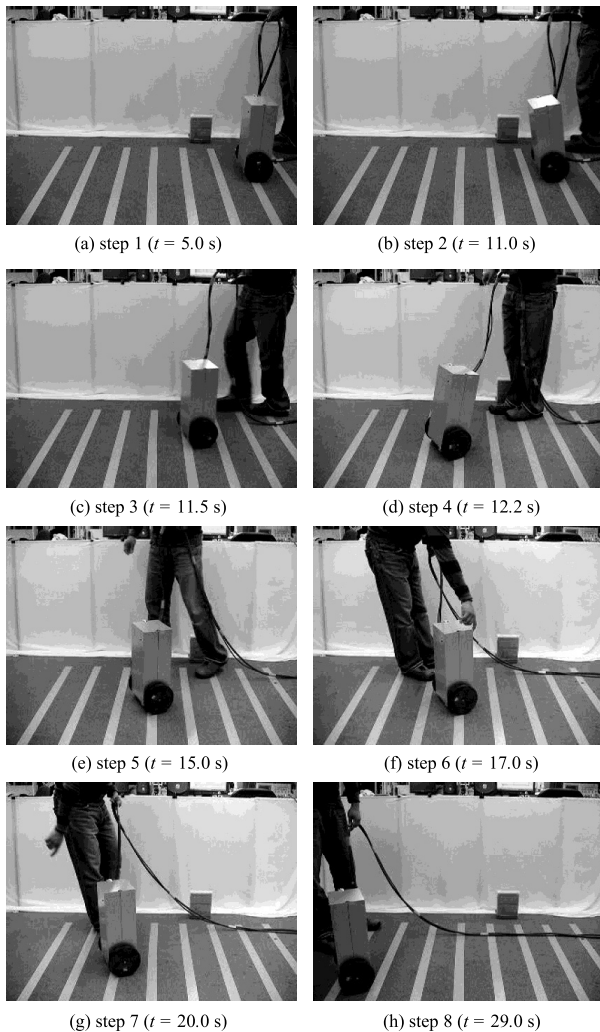


Fig. 10 Sequential photographs of movement control without Kalman filter based disturbance estimate feedback.

#### Akira SHIMADA (Member)



He was born in Chiba, Japan, in 1958. He received the B.S. degree in electronics engineering from the University of Electro Communications, Japan, in 1983 and received the Ph.D. in engineering from Keio University, Japan in 1996. He worked at Seiko Instruments as a robotics engineer from 1983 to 2001. Concurrently, he was a guest professor at Chiba University. He has been an associate professor at the Polytechnic University, Japan since 2001. His current interests include motion control, robotics, and control engineering. He is a member of RSJ and IEEE, and a senior member of IEEJ.

#### Chaisamorn YONGYAI



He was born in Kamphaengphet, Thailand, in 1976. He received the B.S. degree in mechanical engineering from the Polytechnic University, Kanagawa, Japan, in 2003. He is currently pursuing the M.S. degree in mechanical engineering at the Polytechnic University. His current research interests include Kalman filters, disturbance observers and mobile robotics.

- [10] N. Hatakeyama and A. Shimada: Movement control of two-wheeled inverted pendulum robots considering robustness, *Trans. SICE*, Vol.44, No.9, pp.721–728, 2008 (in Japanese).
- [11] M.W. Spong: The swing up control problem for the Acrobot, *IEEE Control Systems Magazine*, Vol.15, No.2, pp.49–55, 1995.
- [12] T. Mita: *Introduction to Nonlinear Control: Skill Control of Under-Actuated Robots*, Syokodo, 2000 (in Japanese).
- [13] Toyota News Release, October 11, 2005.
- [14] C. Yongyai, A. Shimada, and N. Fujii: Kalman filter based disturbance observer and an observation to the use of disturbance estimate, *Proc. 51st Joint Automatic Control Conference*, pp.1226–1231, 2008 (in Japanese).
- [15] A. Shimada, K. Ohishi, M. Shibata, and O. Ichikawa: *EE Text Motion Control*, Ohmusha, 2004 (in Japanese).